THEORETICA CHIMICA ACTA

Theoret. Chim. Acta (Berl.) 61, 105–133 (1982)

Loop Currents in Chlorophyll *a*

Roger E. Clapp

Basic Research Associates, Incorporated, Cambridge, Massachusetts 02138, USA

Loop currents involve the circulation of electrons (or holes) around closed conjugated-bond loops. From the length of the orbital perimeter the kinetic energy per electron can be calculated. In chlorophyll *a*, four electronic excitations have been analyzed, including: (1) a single positive charge (hole) circling a 19-bond orbit with a Möbius twist (this is proposed as the effective ground state); (2) nine electrons, unevenly spaced, circling the same 19-bond orbit but without the Möbius twist (proposed as the red excited state); (3) nine electrons in the same orbit but evenly spaced and vibrationless (the hopping exciton); (4) ten electrons, unevenly spaced, in a 16-bond orbit (the blue excited state). The fit of theory to experiment is examined.

Key words: Chlorophyll – Loop currents – Möbius loops – Photosynthesis – Exciton – Antiparamagnetism.

1. Introduction

Conjugated-bond systems provide topologically-constrained realms within which electrons can move relatively freely. Quantum mechanics imposes restrictions on these movements, specifically the restriction that the wave function for an electron must be continuous. The continuity restrictions limit the acceptable states, and hence the available energy levels. For example, an electron may be free to circulate around a closed orbit formed by a ring of conjugated single and double bonds, so that it can be considered as moving in a toroidal potential well, and its wave function will then be continuous if there is a cumulative phase shift, around one circuit, of any integer multiple of 360°. If the phase shift is 360°, the perimeter of the orbit will be equal to λ, the de Broglie wavelength of this electron. The electron then has a momentum of $p = h/\lambda$, where h is Planck's constant, and a kinetic energy of $p^2/2m_e$, where m_e is the electronic mass.

0040-5744/82/0061/0105/$05.80

This is the free-electron model for electronic excitations in molecules with closed circuits of conjugated bonds. The model has been described in some detail by Platt [1], who points out that there is a demonstrated equivalence among three ways of analyzing these molecules. The three ways are (1) the valence-bond or resonance method, (2) the LCAO (linear combination of atomic orbitals) molecular-orbital method, and (3) the free-electron molecular-orbital method. Early applications to porphyrins are given by Kuhn [2] and Simpson [3], with later work by Gouterman [4, 5]. More recently, extensive treatments of the porphyrins have been presented by Weiss [6] and by Christoffersen [7].

In the latter reference, it is stated that the wave function used for an excited state is a superposition of a large number of separate configurations, where "approximately 300–1300 configurations are used to describe each state". The results obtained can be illustrated by Fig. 1 and Fig. 2, which are taken from Fig. 13 and Fig. 20, respectively, of Christoffersen [7].

Figure 1 treats a relatively simple porphyrin with a high degree of symmetry, and shows a close match between theory and experiment. However, to get this close match it was necessary to introduce a mapping of the calculated transitions

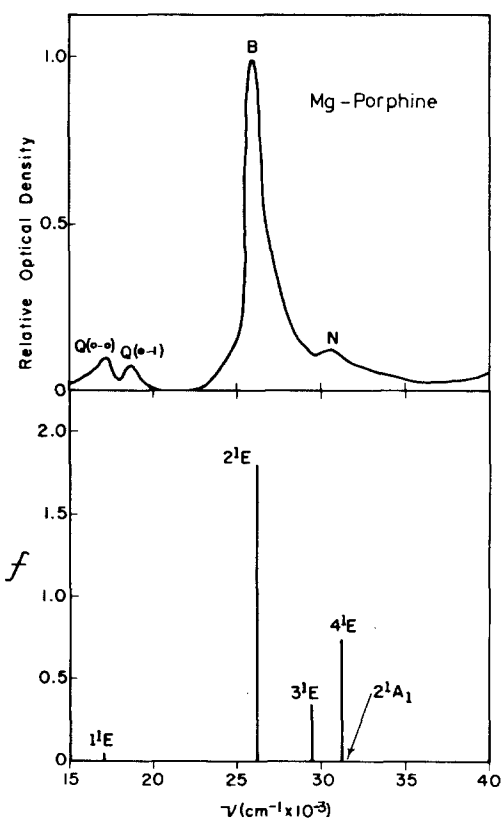

Fig. 1. Experimental absorption spectrum for Mg-etioporphin-1 and calculated spectrum for Mg-porphine by the molecular orbital procedure of Christoffersen [7]. *f* represents the calculated oscillator strength. Reprinted with permission from R. E. Christoffersen, International Journal of Quantum Chemistry **XVI**, 573. Copyright 1979 John Wiley and Sons, Inc.

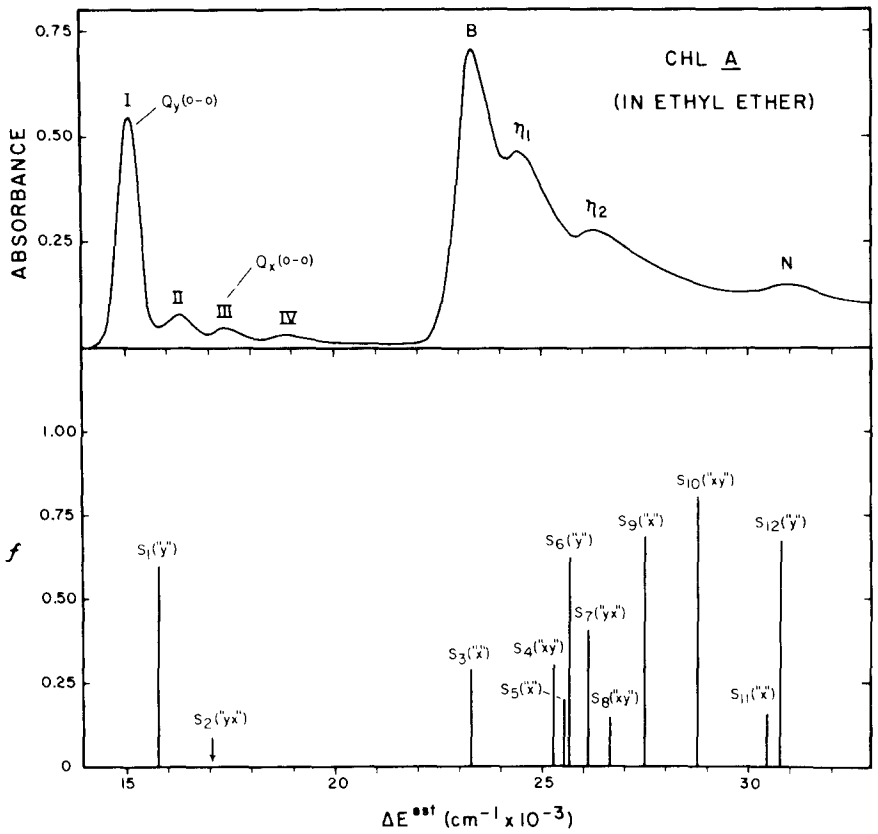

Fig. 2. Experimental absorption spectrum for chlorophyll *a* and calculated absorption spectrum for Et-Chl *a* by the molecular-orbital procedure of Christoffersen [7]. *f* represents the calculated oscillator strength. Reprinted with permission from R. E. Christoffersen, International Journal of Quantum Chemistry **XVI**, 573. Copyright 1979 John Wiley and Sons, Inc.

through the two-parameter relationship

$$\Delta E^{(\mathrm{est})} = 0.610 \Delta E^{(\mathrm{calc})} - 441 \tag{1}$$

where $\Delta E^{(\mathrm{est})}$ and $\Delta E^{(\mathrm{calc})}$ refer, respectively, to estimated and computed Franck–Condon transition energies in units of cm^{-1}. This adjustment of the calculated values, to fit the experimental absorption spectrum, was considered to be justified (on the basis of other studies) due to the small basis set and the limited configuration interaction included in the calculations.

Figure 2 treats the more complicated case which is of interest here, namely chlorophyll *a*, a molecule with a reduced symmetry associated primarily with the reduction of one of the double bonds (in ring IV). The match between the experimental absorption spectrum and the theoretical spectrum, after the transformation in Eq. (1), is less satisfactory. In the Soret region (the right-hand part

of the spectrum), the observed spectrum has more regularity than the calculated spectrum, and has a prominent principal peak which does not stand out in the same way among the many lines included in the calculated spectrum.

The observed spectrum in Fig. 2 can be characterized as "two strong absorption peaks, each having three smaller satellite peaks on the shorter-wavelength side". The calculated spectrum can be characterized as "one strong peak in the red with one very small satellite, and ten scattered peaks in the blue and ultraviolet". It is possible, of course, that further elaboration of the theory would lead to a better match between theory and experiment, but there are already thousands of separate coefficients involved in the calculation. It seems unlikely that further elaboration of this theoretical approach could increase the structure in the red region (the left part of the figure) and *reduce* the structure in the blue and ultraviolet (the right part of the figure). There is thus the possibility that something has been overlooked in the theoretical treatment, something which is important in the biological molecule chlorophyll *a* but is not so important in the non-biological molecule Mg-porphine of Fig. 1.

In the search for what might have been overlooked, I will in this paper go back to the simpler picture embodied in the early free-electron model, but I will generalize this model to allow for the use of wave packets. In this generalization the wave function for a particular electron will be allowed to utilize a superposition of many Hückel orbitals, rather than having to satisfy the restriction of one electron for one Hückel orbital. This added flexibility is an essential new feature. It leads to a "loop-current" picture and permits the inclusion of Möbius orbits which have a key role in what will be presented.

While Möbius orbits have been discussed by Heilbronner [8] and Zimmerman [9], neither of these authors has emphasized that an electron in a Möbius orbit will have an *orbital* angular momentum quantum number which is half-integral. The near-dogma of elementary quantum mechanics allows J to be half-integral but requires L to be an integer. In a Möbius topology, on the other hand, one orbital circuit leaves a pi-electron with its polarity reversed, and continuity of the wave function requires an additional phase shift of an odd multiple of 180°.

That is, an electron which moves in an orbit which rejoins itself with a Möbius twist will be constrained to states which have $L = 1/2,\ 3/2,\ 5/2$, etc. The conventional molecular-orbital expansion does not include such orbits, but the wave-packet generalization which will be used here does permit these Möbius orbits. The topology of the conjugated-bond network in chlorophyll *a* has room for a Möbius orbit, as will be demonstrated, and a Möbius excitation to $L = 1/2$ should be metastable, forbidden to radiate down to $L = 0$. If this is the effective ground state for chlorophyll *a*, as will be suggested, then this molecule would have magnetic properties resembling paramagnetism in the sense that there is a permanent dipole moment, yet resembling diamagnetism in the sense that the moment aligns to oppose the external magnetic field within the orbital ring. The word "antiparamagnetism" is proposed to describe this behavior.

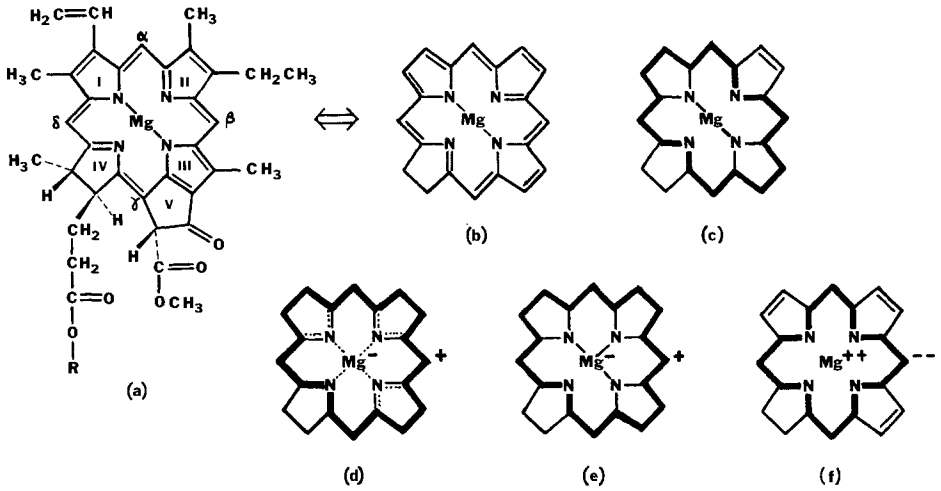

Fig. 3. (**a**) Chlorophyll *a*. The long phytyl chain ($C_{20}H_{39}$) is designated by R. (**b**) The other arrangement of single and double bonds, holding the coordination bonds fixed. (**c**) The combination of (a) and (b) into a diagram showing the electron delocalization as an orbital path. This is structure B of Rabinowitch [10], taken from Fischer [11]. Used by permission. (**d**) Structure D, the low-lying Möbius excitation given in detail in Fig. 4. Partial bonds are shown dotted. (**e**) Structure D*, in which nine electrons circulate around the same 19-bond orbit used by a circulating hole in structure D. (**f**) Structure E^*, in which ten electrons circulate around a 16-bond orbit

2. Möbius Ground State

Figure 3 shows the chemical structure of chlorophyll *a*, including in (a) and (b) two resonating forms differing only in the mesomeric rearrangement of conjugated single and double bonds. These two structures can be combined into the diagram (c), in which the heavy line shows the routing of the conjugated ring, leaving a semi-isolated double bond in nucleus II which does not participate in the conjugation.

This is structure B in the nomenclature of Rabinowitch [10], given in his Formula 16.III, page 442. He also shows two other ways to arrange the magnesium-nitrogen bonds; these arrangements he calls structure A and structure C, placing the semi-isolated double bond in rings III and I, respectively. These three structures were originally introduced by Fischer [11], who argued that structure A should be the more stable. However, the later consensus has settled on structure B, which has become the conventional description.

In Fig. 4, below, I will show another way to get from 3(a) to 3(b), with ionic states participating in the resonance hybrid. Figure 3(d) summarizes this new formulation in which a positive charge circulates around a 19-bond conjugated ring, the heavy line in (d), while a negative charge rests near the center of the structure. Figure 3(e) is an excited state using the same routing, while Fig. 3(f) represents another excited state which uses a different routing and a different charge separation. The excited states are discussed later in the paper.

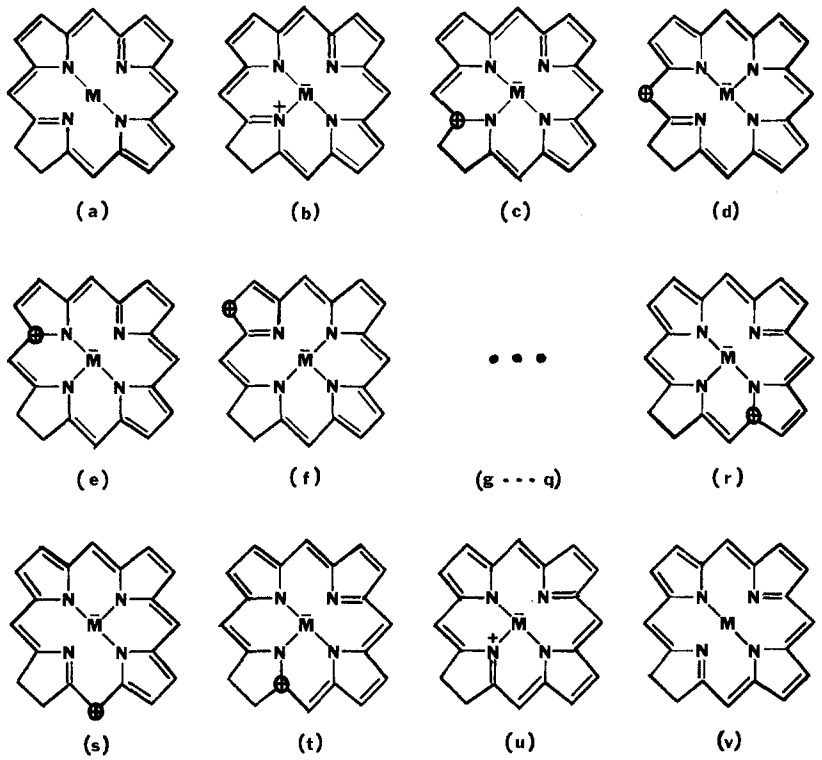

Fig. 4. Positive electronic charge traversing a Möbius orbit, 19 bonds in length, within the porphyrin ring in chlorophyll *a*

In a moderately-sized molecule, there can be participation of many neutral and ionic bonding configurations in a resonance hybrid, representing a particular quantum-mechanical state. In Fig. 4 I show twenty-two such configurations in the inner core of chlorophyll *a*, arranged to display the circulation of a positive charge around the outermost conjugated loop of nineteen bonds. Here I am taking literally the idea of conjugated-bond systems as channels for the movement of electric charge.

I have chosen to follow the motion of a positive charge, an electron "hole," rather than the motion of a single electron, primarily because of the presence of that bottleneck nitrogen atom at the lower left of the ring structure, the nitrogen atom in the partially saturated pyrrole, ring IV. When nitrogen is charged to N^+, it acquires a fourth chemical bond and becomes a temporary carbon, chemically speaking. It then fits more easily into the system of conjugated single and double bonds than would a nitrogen atom charged negatively to N^-. The latter would act as a temporary oxygen with only two valence bonds and would become an obstacle to the movement of pi-electrons through the network.

If a positive charge is to move through the bond network, then its negative balancing charge needs a place to rest. A possible place is the magnesium atom

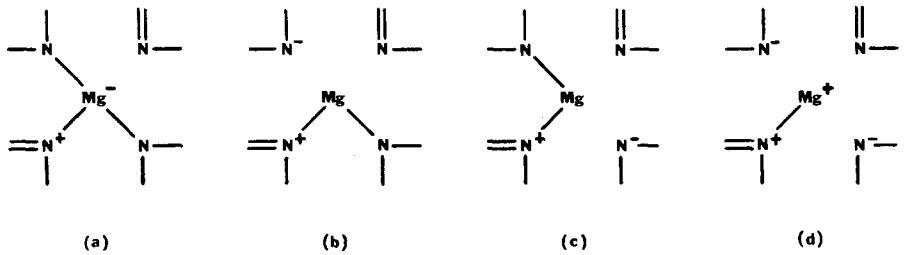

Fig. 5. Delocalization of a centrally resting negative charge, over the magnesium atom and two of the nitrogen atoms

in the center of the ring system. This atom then becomes the negative ion Mg^- which is trivalent and can coordinate with any three of the four nitrogens that surround it. The negative charge could also move onward, to rest on one or another of the nitrogen atoms.

Figure 5(a) shows the negative charge resting on the central magnesium, after moving from the lower left nitrogen leaving the latter positively charged. Fig. 5(b) shows the negative charge moving to the upper left nitrogen. Alternatively, Fig. 5(c) shows the negative charge moving to the lower right nitrogen atom. In Fig. 5(d) there are two divalent N^- ions at upper left and lower right, and a monovalent Mg^+ ion in the center. All four configurations are allowed chemically and can be participating in one resonance hybrid. However, because of the greater electronegativity of nitrogen, relative to magnesium, configurations 5(b) and 5(c) should be dominant over 5(a), and 5(d) could be playing a significant role.

It is most convenient in the diagrams in Fig. 4 to show the negative charge as resting on the central magnesium. But this should be considered as a convenient abbreviation, with the negative charge actually spending much or most of its time on nitrogens.

In Fig. 4, the initial configuration 4(a) is taken directly from Fig. 3(a), and shows the inner skeleton of the molecule, with the central magnesium atom indicated by the single letter M. For configuration 4(b), an electron is moved from the lower left nitrogen to the central magnesium. These are then denoted by $\dot{\bar{N}}$ and $\bar{M}$, where $\bar{M}$ is intended to represent a resonance as depicted in Fig. 5.

There are two other ways of arranging bonds which will leave the immediate surroundings of the positive charge in Fig. 4(b) unaltered. These involve the shifting of the open nitrogen-magnesium connection. In 4(b), this open connection involves the upper right nitrogen; in the two alternative arrangements, this open connection is shifted to the upper left and lower right nitrogens, respectively. When we include these two alternative arrangements of coordination bonds (and associated rearrangements of single and double bonds), we can attribute a multiplicity of three to the configuration 4(b).

In Fig. 4(c), the positive charge has moved to the other end of the double bond in 4(b), leaving the *N* atom now neutral and trivalent. The network carbon to

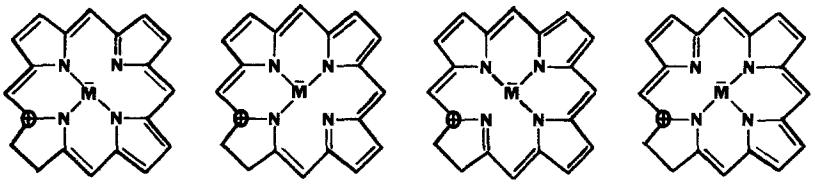

Fig. 6. Four ways of arranging bonds, compatible with the location of the mobile positive charge in the position specified in Fig. 4(c)

which the positive charge has moved is now a trivalent C^+ ion, denoted by a plus sign in a small oval. The multiplicity is four, as spelled out in Fig. 6.

The conjugated-bond system does not extend to the two outer carbons in the partially-saturated ring IV. There is therefore no option for the next step; the positive charge must move upward toward the δ-carbon at the middle left of the porphyrin ring. This motion, together with an associated bond rearrangement, leads to configuration 4(d). While the energy needed for this configuration is about the same as for configuration 4(c), the multiplicity is reduced from four to one, since there are no other low-energy bondings that will place the positive charge in the location shown in 4(d). This low-multiplicity step in the positive-charge progression can therefore be considered as a gentle obstacle to the forward motion, but not a serious obstruction.

In Fig. 4(e) the positive charge has moved upward one more step. The bond configuration shown here is only one of four different configurations of about the same energy, differing in the location of the omitted nitrogen-magnesium coordination bond. That is, the multiplicity to be associated with the configuration 4(e) is four. And each of these four bond rearrangements is further subject to the delocalization of the negative charge as illustrated in Fig. 5.

In the further steps of Fig. 4, the positive charge moves from one location to the next around the outermost available orbit within the conjugated-bond system. Configurations 4(g) through 4(q) are not shown explicitly, but can be filled in by the reader. Each stage is a valence-bond representation of the momentary electronic configuration, compatible with a specified location of the positive charge. In most cases, the representation is exemplary, is one possible bond configuration among two to four resonant alternatives. When we include the available low-lying configurations, we find that the 20 configurations 4(b) through 4(u) actually involve 54 available bond arrangements, and this is before the inclusion of the delocalization of the central negative charge, as illustrated in Fig. 5.

These resonating configurations with the stepped forward motion of the positive charge should be thought of as a valence-bond picture of a continuous process in which there is the movement of one positive charge around an orbital path. Simultaneously there are readjustments of the remaining electron distribution to maintain the best bonding, the greatest degree of joint occupation of local quantum states by pairs of electrons with opposite spins.

When configuration 4(t) has been reached, the positive charge is ready to move to the lower left nitrogen atom. To do this, it needs to use a nitrogen pi-electron whose phase is reversed relative to the phase of the nitrogen pi-electron involved in the double bond in configuration 4(b).

This is an important point. When there are truly alternating single and double bonds, as for example in cyclo-octatetraene, one atom which is linked between two others will have a pi-electron whose wave function is phased to match the phasing of the pi-electron on the next atom to one side, and to counter the phasing on the next atom to the other side. On the side with the match there is a double bond. On the side with the mismatch there is a single bond. If the pi-electron on the central atom is reversed in phase, so that the plus and minus lobes of its figure-eight wave function are interchanged, then this inner pi-electron will lean the other way. It will repel the adjacent pi-electron to which it was previously bonded, and it will be drawn to the pi-electron on the other side, which it had previously repelled.

That is, the double and single bonds will have been interchanged as a result of the phase reversal of the pi-electron on the central atom. In cyclo-octatetraene the phase reversal of four pi-electrons, on the clockwise side of each double bond, will have the effect of interchanging double and single bonds.

When the positive charge moves from 4(t) to 4(u), it can be considered to rejoin its own wave function, but upside-down, with a 180° phase reversal. This is a Möbius-loop junction. A similar Möbius orbit would result if a pi-electron progression involved a succession of tilts of the pi-electron figure-eight wave function, accumulating to a 180° tilt in orientation angle over one traversal of the orbit. Such Möbius orbits have been described by Heilbronner [8] and are discussed also in the textbook by Zimmerman [9].

The junction in Fig. 4(u) contains a topological phase reversal, and would by itself represent a discontinuity in the orbital wave function, but if the wave function has accumulated a phase shift which is an odd multiple of 180° then this junction can have the needed continuity. The cumulative phase shift will compensate for the topological phase reversal. What this means is that the circulating positive charge needs to have half-integral *orbital* angular momentum, with $L = 1/2$, or $3/2$, or $5/2$, etc.

In Fig. 4 the final step to configuration 4(v) has carried the molecule from the bond structure of Fig. 3(a) to the complementary structure of Fig. 3(b). However, if we halt at 4(u), then introduce a bond rearrangement involving eighteen bonds in a loop, the loop of structure B, Fig. 3(c), a rearrangement which can be accomplished through the reversal of phase of nine pi-electrons but with no phase reversal of the mobile positive charge, then we have once again the configuration 4(b) and the orbital motion can continue.

With a continuing orbital motion, in which the momentum associated with the moving positive charge has the magnitude to give a 180° phase shift over each orbit, we find that the perimeter of the orbit needs to be equal to $\lambda/2$, where λ

is the de Broglie wavelength of the moving entity. This entity is here a positive charge, but the steps forward by the positive charge can actually be accomplished by the stepped motion of negative charges moving in the opposite direction. For the hole to move forward, a physical electron moves in the other direction, filling the location of the hole while opening up a space which is one step down the line. This opened space then becomes the new location for the moving positive charge. In engineering terms, this is a "backward wave".

We can estimate the orbital perimeter as the sum of two C—N bonds of length 1.42 Å each, plus seventeen C—C bonds of length 1.40 Å each, giving 26.64 Å as the total. The de Broglie wavelength is then $\lambda = 53.28 \cdot 10^{-8}$ cm, and the associated kinetic energy is

$$\frac{h^2}{2\lambda^2 m_e} = 0.85 \cdot 10^{-13} \text{ erg} \tag{2}$$

This energy is about twice the thermal energy kT for $T = 300°\text{K}$. If we neglect associated potential energies, and treat (2) as the energy difference between this $L = 1/2$ state and a lower $L = 0$ state, then decay is *energetically* probable at ordinary temperatures.

However, *radiative* decay from $L = 1/2$ to $L = 0$ is forbidden, and other modes of energy coupling, such as lattice vibrations in the surrounding medium, may be only very weakly coupled to this electronic transition. The Möbius excitation will have a particular sense of charge circulation, which could be reversed by a radiative interaction, but this would be a transition from $L = 1/2$ to $L = 1/2$ and would leave the molecule still carrying the kinetic energy in Eq. (2).

In photosynthetic plants the active chlorophyll molecules are bound to membranes with the porphyrin ring systems oriented parallel to the planes of the stacked membranes. In a strong magnetic field it is observed [12–16] that the membranes in chloroplasts align perpendicular to the magnetic vector. This observation might be evidence that the molecules are paramagnetic, with each magnetic moment perpendicular to the plane of the porphyrin ring. That is, each chlorophyll *in vivo* could be in a metastable Möbius electronic excitation which was serving as the effective ground state.

There is independent evidence from nuclear magnetic resonance (NMR) that the protons in chlorophyll are shielded in some cases, "deshielded" in others, by "ring currents" within the network of conjugated bonds, when the chlorophyll molecules are in a strong magnetic field. This effect, leading to chemical shifts in the proton NMR signals, has been explained [17, 18] as a diamagnetism resulting from the ring currents induced by the external magnetic field. Diamagnetism by itself would tend to align the molecular planes parallel to an external magnetic field, as pointed out [19] by experimenters measuring the orientation of DNA chains in a magnetic field.

With paramagnetism there is a permanent magnetic moment which is oriented in an external magnetic field. With diamagnetism there is an induced magnetic

moment which is created by the external magnetic field. When the paramagnetism is itself associated with a loop current, the sense of that current could be with or against the external field, and if it is in the direction to counter the field then it would mimic the diamagnetic ring currents, yet its permanence would act to align the chloroplast membranes perpendicular to the field. So loop currents might explain both the NMR chemical shifts and the observed membrane orientations. An appropriate name for this negative paramagnetism might be "antiparamagnetism".

In marshalling evidence for a Möbius effective ground state, we can make a further argument, based on biological function. In living chloroplasts, chlorophyll is organized into "photosynthetic units". Each photosynthetic unit consists of several hundred monomer chlorophylls, called "antenna" chlorophylls, and one reaction center in which the chlorophyll is in dimer form or in more elaborate polymeric associations. A solar photon is collected by one antenna chlorophyll and converted to an "exciton" which hops from one antenna to another, *never fragmenting*, until it reaches the reaction center where its free energy is utilized in biochemical reactions of energy storage and the building of sugars.

A possible model for the exciton, to be discussed later, has nine electrons circulating around the 19-bond orbit of Fig. 3(e), carrying a high angular momentum but no vibrational energy, carrying a magnetic dipole moment and an associated magnetic field distribution but no electric dipole moment. For a solar-excited state to convert readily to such an exciton, *it also* should contain a circulating electrical current flow. There is indeed evidence from magnetic circular dichroism in related molecules, suggesting that the porphyrin ring can carry circulating electrical currents of large magnitude.

A particular example is shown in Fig. 7. The molecule here is chlorin-e_6 trimethyl ester, and the measurements are those reported by Briat et al. [20]. What is shown is the absorption spectrum (dashed), the CD (circular dichroism) spectrum (dotted), and the MCD (magnetic circular dichroism) spectrum. The MCD spectrum is the one of particular interest here. The externally applied magnetic field of 41.7 kilogauss is directed parallel to and in the sense of the direction of propagation of an incident beam of plane-polarized monochromatic light. The light emerging from the interaction with the molecules has acquired an ellipticity angle θ which is measured and compared with the ellipticity which is introduced by the molecules in the absence of the magnetic field. The difference is what is plotted as the solid curve in Fig. 7.

The acquired ellipticity of the emerging light is a result of a difference in the absorption of the sample for right-handed and left-handed circulatory-polarized light. This difference is here correlated with the direction of the externally applied magnetic field. The resulting signal is very large in this case, particularly in the Soret region around 400 nm (25 000 cm^{-1}).

A full explanation of the detailed spectra shown in Fig. 7 is likely to be very complex, and no such explanation will be undertaken here. However, the very

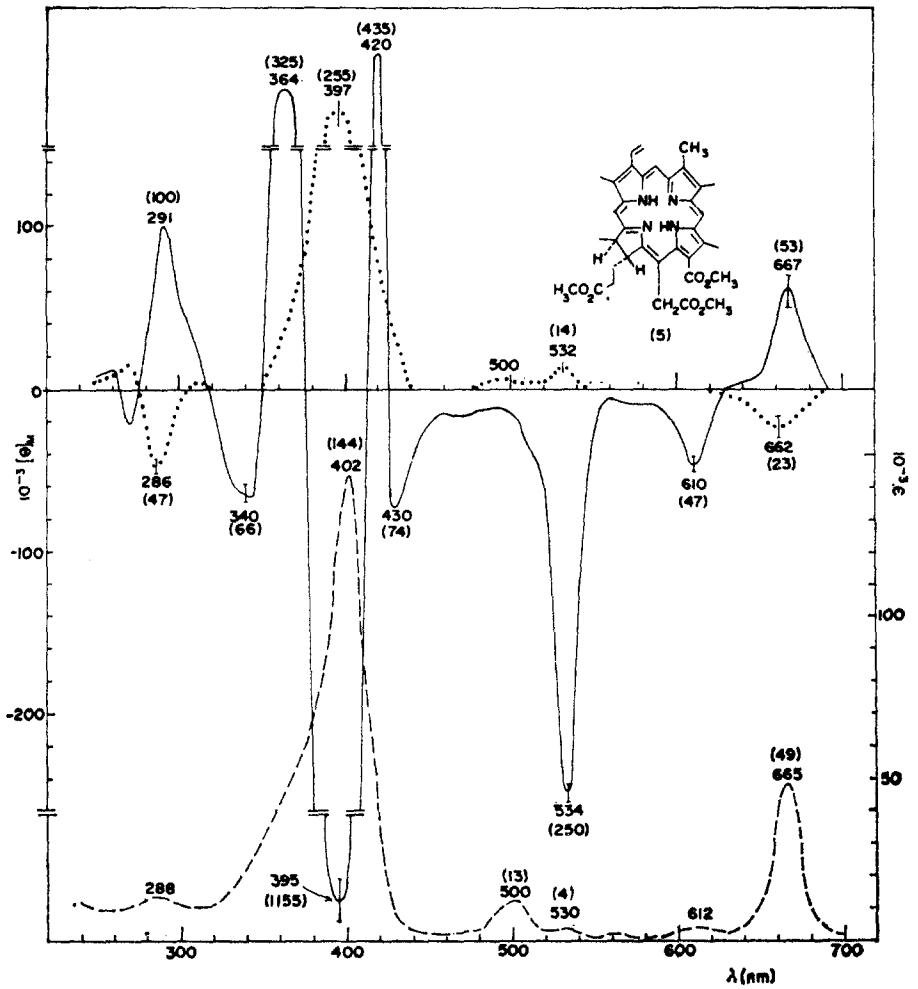

Fig. 7. Absorption (– – – –), circular dichroism (· · · ·), and magnetic circular dichroism (———) of chlorin-e_6 trimethyl ester. Reprinted with permission from Briat et al., J. Am. Chem. Soc. **89**, 6170. Copyright 1967 American Chemical Society

magnitude of the MCD effect, as shown for example in the negative peak of 1155 units, at 395 nm, can be considered as evidence for a strong circulation of electrical current around the conjugated-bond network, in a direction specified in advance by the external magnetic field.

The advance specification could be through the orientation of the ground-state molecules, if these are actually in an antiparamagnetic state with a positive charge circulating in a Möbius orbit. The strong external magnetic field would then tend to align the molecules with their ground-state circulation preferentially countering the external field. The selection rules for radiative excitation would

choose the direction of circular polarization which a particular molecule could respond to, based on its ground-state orientation. In this way the magnetic field would set the ground states, and this in turn would select the sense of circular polarization to be absorbed, and we would see this as a MCD measurement. But there are still other phenomena dealing with ground-state magnetism in the molecules of chlorophyll *a*.

In freeze-fracture electron microscopy studies of chloroplasts, it is found that the molecules in a photosynthetic unit cling together in a clump [21]. This might be evidence that the antenna chlorophylls are coupled together magnetically, with their antiparamagnetic vectors all pointing in the same direction. The polarity of the effective ground state then specifies the polarity of the excited state that results from the absorption of a red or blue solar photon, and therefore the polarity of the exciton that is generated. If the dimeric structure or structures in the reaction center contain a magnetic moment of the opposite polarity, then this could tend to draw the hopping exciton inward toward the reaction center, an element of efficiency that would be of considerable advantage in evolutionary competition against photosynthetic organisms that depended on random hopping to bring the exciton to the reaction center.

There are two kinds of photosynthetic unit, allocated to "Photosystem I" and "Photosystem II". In the former, the simpler of the two, only chlorophyll *a* appears among the antenna chlorophylls, and the reaction center includes a dimer of chlorophyll *a*. This reaction center has been called P700, from its optical absorption peak near 700 nm. When cooled to liquid nitrogen temperatures (about 77°K), this reaction center shows a fluorescence [22] peak at 735 nm, not present at ordinary temperatures except for a brief fluorescence lasting only about 80 picoseconds [23]. This reaction center is known to contain a chlorophyll dimer, through electron spin resonance measurements showing that there is an unpaired electron delocalized over a doubled volume [24], once the processing of an exciton has led to the ejection of a high-potential electron carrying the bulk of the free energy to be processed.

The observations just described can be interpreted in terms of Möbius loop currents in the chlorophyll dimer. The delocalization shows that the two porphyrin rings are electronically connected. The circulation of two positive charges over the two rings in a long Möbius orbit would have a kinetic energy about one-half of that given in Eq. (2). If this excitation is the "prepared" ground state of the dimer *in vivo*, then there should be an excited state at a level which is reached by a photon of about 700 nm wavelength.

The separation between the prepared ground state and the excited state then would explain the absorption peak of the reaction center P700. Now if in addition there is an "elevated" ground state in which there are two (Möbius) positive charges circulating separately around the two porphyrin rings, the associated kinetic energy would be roughly twice the value in Eq. (2). An excited state reached from this elevated ground state, and re-emitting by fluorescence, would give rise to a fluorescent peak in the vicinity of 735 nm, if the excited state

contained about the same energy as the excited state reached from the prepared ground state.

The elevated ground state, with its two independent Möbius excitations, would have more entropy, obviously, than the prepared ground state with its coupled-pair Möbius excitation. The lowering of the reaction center from the former to the latter state would require the emission of energy and entropy. The energy needed is close to the energy of a 15-micron photon in the infrared, and the entropy to be disposed of is probably substantially less than the entropy carried by a black-body photon. (Clapp [25] has calculated that the average entropy carried by a black-body photon is $2.7012k$, where k is Boltzmann's constant.)

From the arguments above, it would seem that there are important roles that Möbius ground states could be playing in the phenomena of photosynthesis. New experiments could clarify these roles, particularly experiments designed to measure emission from the reaction centers of Photosystem I, in the infrared neighborhood of 15 microns. A particular experiment, to examine whether illumination at 15 microns will enhance or quench the 735 nm fluorescence at 77°K, has been proposed [25]. The quenching would be by a process of stimulated emission which shortened the time which a reaction center P700 spent in the elevated ground state, before moving to the prepared ground state to await another exciton.

There is ample experimental evidence of low-lying optically-forbidden excitations in substituted benzenes [26]. These might involve Möbius excitations of the benzene ring. The measurement technique, using threshold-electron-excitation (TEE) spectra [27], is at present not sensitive enough to detect Möbius excitations in porphyrins, but future improvements in resolution are of course possible.

3. Explicit Wave Functions

The orbital circulation of Fig. 4 is summarized in structure D, shown in Fig. 3(d). Let us map the 19-bond orbit, the heavy line in Fig. 3(d), onto the unit circle, so that once around takes us from $\theta = 0°$ to $\theta = 360°$, or from 0 to 2π in radian measure.

We can take the nitrogen atom in the orbit as the zero reference point. There are then 19 atomic locations around the orbit, almost equally spaced, with their radian positions specified approximately by

$$\theta_n = 2\pi n/19, \qquad n = 0, 1, 2, \ldots, 18. \tag{3}$$

The initial position, $\theta_0 = 0$, is the lower left nitrogen atom.

An electronic wave function over this re-entrant one-dimensional space will be a function of θ, and may also be a function of the time t if a moving particle is being described. Consider the set of wave functions

$$\psi_n(\theta_t) = F_n(\theta_t) \exp(i\theta_t/2) \tag{4}$$

where θ_t is defined by

$$\theta_t = \theta - \omega t \tag{5}$$

and ω is the radian frequency for the orbital motion. The amplitude factors F_n are here defined by

$$\begin{aligned} F_n(\theta_t) &= \frac{\sin[19(\theta_t - \theta_n)]}{38 \sin[(\theta_t - \theta_n)/2]} \\ &= \tfrac{1}{19}\{\cos[(\theta_t - \theta_n)/2] + \cos[3(\theta_t - \theta_n)/2] \\ &\quad + \cdots + \cos[37(\theta_t - \theta_n)/2]\}. \end{aligned} \tag{6}$$

The nineteen amplitude factors F_n are plotted in Fig. 8. Their Möbius character is evident, in that a displacement of 2π along any curve results in a phase-reversed waveform, an inverted replica. The localization to the dimension associated with one network atom is also evident.

These amplitude factors are all mutually orthogonal, satisfying the orthogonality conditions

$$\int_{\theta_t=0}^{\theta_t=2\pi} F_m(\theta_t) F_n(\theta_t)\, d\theta_t = 0, \qquad m \neq n. \tag{7}$$

This orthogonality then leads to the Hermitian orthogonality of any pair of wavefunctions ψ_m and ψ_n, as defined in Eq. (4).

Each wave function (4) can be seen to be a linear combination of 38 Hückel orbitals, each progressing around the loop at the radian frequency ω. In particular,

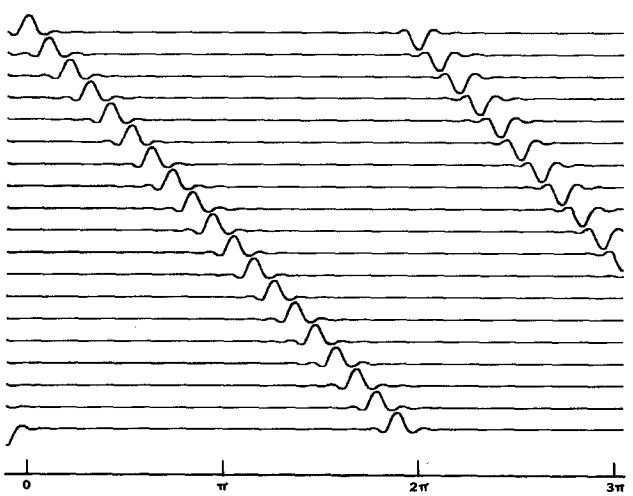

Fig. 8. The wave-function amplitudes F_n for nineteen orthogonal Möbius orbitals within the orbit of structure *D*, Fig. 3(d)

consider $\psi_0(\theta_t)$, which can be written in the expanded form

$$\psi_0(\theta_t) = \tfrac{1}{38}[\exp(-18i\theta_t) + \exp(-17i\theta_t) + \exp(-16i\theta_t) + \cdots + \exp(18i\theta_t) + \exp(19i\theta_t)]. \quad (8)$$

These 38 Hückel orbitals do not correspond here with 38 electrons, but with 38 contributions to the wave function of one electron, or in this case one missing electron, one positive charge, one "hole".

The backward-wave circulation of one positive charge, as noted earlier, keeps just one physical electron in motion at any one moment. We can also consider a forward-wave movement, in which a positive charge is carried around the orbit through the simultaneous forward movement of many electrons, with the positive charge just manifested as a gap in the sequence of negatively-charged electrons.

Specifically, let us consider a forward-wave circulation in the nineteen-bond orbit of Fig. 3(d) where we now leave nine pi-electrons at rest, all with "spin up", while nine other pi-electrons, all with "spin down", circle the orbit in a forward wave in which each electron moves in a non-Möbius loop in which $L = 1$. This forward-wave excitation is designated as structure D^*, shown in Fig. 3(e).

Explicit wave functions for this forward-wave excitation are suggested in Fig. 9. Nine electronic wave functions are shown, selected from the set

$$\psi_j(\theta_t) = G_j(\theta_t) \exp(i\theta_t) \quad (9)$$

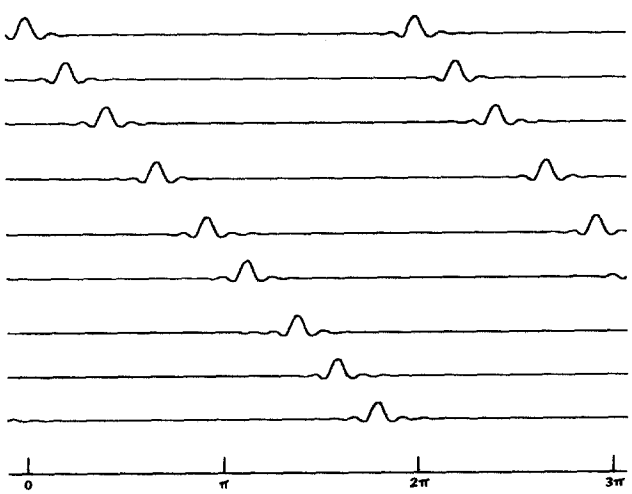

Fig. 9. The wave-function amplitudes G_j for $j = 0, 4, 8, 13, 18, 22, 27, 31, 35$. These are non-Möbius orbitals within the orbit of structure D*, Fig. 3(e)

where θ_t is as given earlier in Eq. (5). The amplitude factors G_j are defined by

$$G_j(\theta_t) = \frac{\sin[39(\theta_t - \theta_j)/2]}{39 \sin[(\theta_t - \theta_j)/2]}$$
$$= \tfrac{1}{39}\{1 + 2\cos(\theta_t - \theta_j) + 2\cos[2(\theta_t - \theta_j)]$$
$$+ \cdots + 2\cos[19(\theta_t - \theta_j)]\} \tag{10}$$

where the θ_j are here defined by

$$\theta_j = 2\pi j/39. \tag{11}$$

Within this set there are 39 orthogonal functions available. Figure 9 shows nine of the amplitude factors, G_j, the nine for which $j = 0, 4, 8, 13, 18, 22, 27, 31, 35$.

You will note that I have left three gaps of 4, clustered closely together, among the six gaps of 3. This spacing has been chosen to make the gaps appear to a photon as a circulating half-positive charge, $q = 1/2$, in an orbital state with $L = 1$. The product, $qL = 1/2$, is to be compared with the effective ground state in which one positive charge circulates in an orbit with $L = 1/2$, with $qL = 1/2$ as the result.

From $qL = 1/2$ to $qL = 1/2$ can be a permitted radiative transition, $\Delta(qL) = 1$, provided that the direction of circulation of the positive charge is reversed. Since the transition is from backward wave to forward wave, a reversal in qL leads to an accentuation in the circulation of physical electrons around the porphyrin ring.

The de Broglie wavelength associated with each of the nine electrons will equal the orbital perimeter, $26.64 \cdot 10^{-8}$ cm, rather than twice the perimeter (as was the case for the Möbius excitation), and the kinetic energy per electron will be four times the value in Eq. (2), or $3.40 \cdot 10^{-13}$ erg. There are now nine electrons in simultaneous motion, so the total kinetic energy is about $30.60 \cdot 10^{-13}$ erg. The transition energy between the Möbius effective ground state and the nine-electron excited state will include a kinetic energy contribution of $29.75 \cdot 10^{-13}$ erg. Some electrostatic potential energy can be associated with the charge separation which places a positive charge on the outer 19-bond ring and a negative charge on the magnesium and nitrogens, but this energy contribution should be about the same for the ground state and excited state, hence should contribute little to the transition energy. There should be some magnetic potential energy coupling the current loop to the magnetic moment of the inner negative charge, and some vibrational energy associated with the uneven current flow, but if we neglect the magnetic and vibrational contributions we find that the transition energy matches the energy of an optical photon with the wavelength

$$\lambda_{\text{red}} = 668 \text{ nm}. \tag{12}$$

Including the vibrational shaking of the structure, associated with the compactness and uneven spacing of the electronic wave functions in Fig. 9, would shorten this optical wavelength. The observed red peak for chlorophyll *a* dissolved in

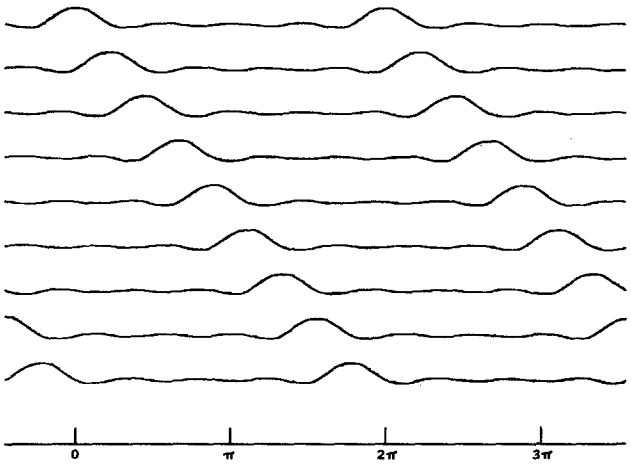

Fig. 10. The wave-function amplitudes H_k for $k = 0, 1, 2, 3, 4, 5, 6, 7, 8$. These are relaxed non-Möbius orbitals within the orbit of structure D*, Fig. 3(e)

acetone is given by Seely [28] as 662 nm. The agreement with Eq. (12), allowing for a vibrational contribution, is very close.

We can expect that the vibrational energy will be quickly emitted as a phonon or phonons into the fluid medium around the chlorophyll molecule by a relaxation process which does not alter the electronic current flow. The lowest such relaxed state is shown in Fig. 10. Here the nine electrons are smoothly and evenly spaced around the 19-bond loop. Each is described by one of the nine wave functions

$$\psi_k(\theta_t) = H_k(\theta_t) \exp(i\theta_t) \tag{13}$$

where θ_t is as given in Eq. (5), where $k = 0, 1, 2, \ldots, 8$, and where H_k and θ_k are defined by

$$\begin{aligned} H_k(\theta_t) &= \frac{\sin[9(\theta_t - \theta_k)/2]}{9 \sin[(\theta_t - \theta_k)/2]} \\ &= \tfrac{1}{9}\{1 + 2\cos(\theta_t - \theta_k) + 2\cos[2(\theta_t - \theta_k)] \\ &\quad + 2\cos[3(\theta_t - \theta_k)] + 2\cos[4(\theta_t - \theta_k)]\} \end{aligned} \tag{14}$$

$$\theta_k = 2\pi k/9. \tag{15}$$

What is shown in Fig. 10 is the set of nine amplitude functions H_k.

There is Hermitian orthogonality between any pair of the thirty-nine wave functions (9), and there is Hermitian orthogonality between any pair of the nine wave functions (13). Any one of the wave functions (9) is a linear combination of 39 Hückel orbitals, while any one of the wavefunctions (13) is a linear combination of 9 Hückel orbitals. In particular, the first of the wave functions

(13) has the expanded form

$$\psi_0(\theta_t) = \tfrac{1}{9}[\exp(-3i\theta_t) + \exp(-2i\theta_t) + \exp(-i\theta_t) + 1 + \exp(i\theta_t) + \exp(2i\theta_t) + \exp(3i\theta_t) + \exp(4i\theta_t) + \exp(5i\theta_t)]. \quad (16)$$

The other eight of the wave functions (13) are similar expansions with nine terms, but the numerical coefficients are various arrangements of the complex ninth roots of unity. The wave function (16) and the other eight of the wave functions (13), taken together, can be treated as a Hückel assembly in which there has been the lifting of one electron from the $\exp(-4i\theta)$ orbital to the $\exp(+5i\theta)$ orbital. Since in this case there are only nine Hückel orbitals involved in the description of the wave functions for nine electrons, there is a relatively close correspondence between the loop-current picture (the number of Hückel functions may be much larger than the number of electrons) and the conventional Hückel picture (the number of Hückel functions equals the number of electrons).

Let us look at the charge-density distribution for the assembly (13) of nine moving electrons, shown in Fig. 10. When we take the magnitude-squared of each wave function, then add these charge densities together, we find that we have a constant (equal to unity) which is independent of the position around the orbit. That is, the charge is evenly distributed around the orbit.

There is a current flow around the orbit, carrying kinetic energy and an associated magnetic field, but electrically this is a static magnetic dipole with no oscillating electric dipole moment. This magnetic-dipole excitation is my proposal as the "exciton" of Photosystem I in green plants. I can see this loop-current energy being coupled from one antenna chlorophyll to the next, with the magnetic lines of force linking the two rings as in a one-to-one electrical transformer. I can see the hopping progressing preferentially toward the nearest PSI reaction center, where there could be an effective ground state containing an electrical circulation with a polarity that magnetically drew the excitation inward toward the reaction center.

Most particularly, I can see why this exciton can never fragment. The nine circulating electrons (Fig. 10) form a quantum-mechanical structure with $L = 9$, but this structure is electrically so balanced that there is no fluctuating electrical charge density that can couple to a lower-lying state to give rise to radiation.

The state with $L = 9$ has no accessible method of fragmenting, and hops without fragmenting until it reaches the reaction center. Here its free energy is processed, converted into the stored energy in a sugar molecule. The excess entropy which accompanied the solar photon's energy must be disposed of, but this is a side issue which I discuss in detail elsewhere [25].

For the present discussion, I will concentrate on just four different electronic excitations within the molecular structure of chlorophyll *a*. These include the Möbius excitation which I propose as the effective ground state, the nine-electron

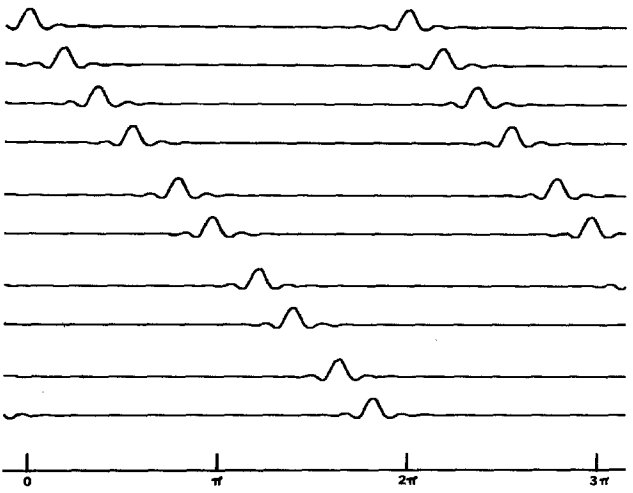

Fig. 11. The wave-function amplitudes $E_{j'}$ for $j' = 0, 3, 6, 9, 13, 16, 20, 23, 27, 30$. These are non-Möbius orbitals within the orbit of structure E*, Fig. 3(f)

red excited state shown in Fig. 9, the relaxed exciton shown in Fig. 10, and a blue excited state which I show here in Fig. 11.

There are ten electrons shown in Fig. 11. These are considered to circulate around the sixteen-bond loop shown as the heavy line in structure E^*, Fig. 3(f). For this mode of excitation, I have considered that the eight pi-electrons with one spin direction, already present in the sixteen-bond loop (the most symmetrical loop available within the conjugated-bond system), can be augmented by two more electrons taken from the magnesium atom in the center. This atom becomes the doubly-charged ion Mg^{++}.

The circulating electrons in Fig. 11 have wave functions defined by:

$$\psi_{j'}(\theta_t) = E_{j'}(\theta_t) \exp(i\theta_t) \tag{17}$$

$$E_{j'}(\theta_t) = \frac{\sin[33(\theta_t - \theta_{j'})/2]}{33 \sin[(\theta_t - \theta_{j'})/2]}$$

$$= \tfrac{1}{33}\{1 + 2\cos(\theta_t - \theta_{j'}) + 2\cos[2(\theta_t - \theta_{j'})]$$

$$+ \cdots + 2\cos[16(\theta_t - \theta_{j'})]\} \tag{18}$$

$$\theta_{j'} = 2\pi j'/33. \tag{19}$$

Figure 11 shows the ten amplitude factors $E_{j'}$ for $j' = 0, 3, 6, 9, 13, 16, 20, 23, 27, 30$. There are three gaps, each representing one-third of a positive electronic charge, positioned after the fourth, sixth, and eighth electrons. Spaced out in this way, their centroid is moved inward so that when referred to the actual radius of the orbit they have a combined effective charge strength of 0.49, roughly one-half positive charge. As with the excitation of Fig. 9, this ten-electron

excitation should appear to a photon as a half-positive charge circling an orbit with $L = 1$, an excited state with $qL = 1/2$.

The transition from the Möbius ground state should be an allowed radiative transition. The kinetic energy associated with this ten-electron excited state can be computed from the orbital perimeter of 22.56 Å, and has the magnitude of $47.34 \cdot 10^{-13}$ erg. The electrostatic potential energy could be comparable to that for the Möbius ground state, since there are now two charge pairs instead of one but these are separated by about one-half the distance. If we omit the contributions of vibration and of electric and magnetic potential energies, then we find a transition energy of $46.49 \cdot 10^{-13}$ erg, which corresponds to a blue photon with the wavelength

$$\lambda_{\text{blue}} = 427 \text{ nm}. \tag{20}$$

This is not far from the observed absorption peak at 430 nm (Seely [28]).

In green plants, the full energy of the absorbed blue photon is not passed on directly to the reaction center. There is an immediate conversion of the excitation to the lower-energy exciton, the same exciton that results from the absorption of a red photon. Comparison of Fig. 3(f) with Fig. 3(e) shows that the conversion must be more than a simple vibrational relaxation. Furthermore, the energy difference to be disposed of, about $17 \cdot 10^{-13}$ erg, is far above the thermal energies in the phonon spectrum at biological temperatures. It seems probable that evolutionary competition would have favored those organisms that found ways to store for later utilization the energy differential between the blue excitation and the nine-electron exciton. One possibility is an optically forbidden excitation of electrons circulating back and forth along the polyene chain of a carotenoid; there are always carotenoids in association with chlorophyll in photosynthetic organisms.

4. Satellite Peaks

I have focused attention on two specific excited states, a 9-electron loop current in a 19-bond orbit and a 10-electron loop current in a 16-bond orbit. In these instances the kinetic energies of the circulating electrons appear to be sufficient to account for the observed absorption energies (for the main red and blue peaks in the absorption spectrum for chlorophyll *a*). Potential-energy contributions have been discussed, but some are positive and some are negative, and evidently there is a balancing of these, so that the absorbed energy from the incident photon is converted almost directly into kinetic energy of electron motion.

We can consider other excited states of similar character. For example, in the 19-bond orbit we have 9 circulating electrons and 9 other pi-electrons which are at rest. (The nineteenth pi-electron has moved to the center of the molecule.) If more energy is incident, it could place 10 electrons in the circulating set, leaving only 8 at rest. The kinetic energy would be increased, but there would be some compensating potential energy, since now each of the 10 moving

electrons will be moving through a channel containing one less stationary electron, hence one more positive charge. This is a deeper channel.

With more incident energy, the circulating set can be 11 electrons, or 12 electrons. Added kinetic energy is required, but partial compensation comes from the deeper potential well that results when electrons are shifted from the stationary set to the moving set. Countering this deepening potential well is the mutual repulsion between the moving electrons. As more electrons are shifted to the circulating set, these become more crowded together, and their mutual repulsion becomes more important.

A similar situation can apply to the 16-bond orbit. While the 10-electron loop current appears to convert all the "blue" photon energy into circulating kinetic energy, we can also consider excitations in which there are 11, 12, or 13 electrons moving in this orbit. The added kinetic energy will be partially compensated by the deepening potential well, but this compensation will be countered by the repulsion between the moving electrons. Here we need to allow for potential-energy contributions, since the observed satellite peaks (see Fig. 2) do not exactly match the calculated positions obtained from kinetic energies alone.

For the circulating electrons to move freely through the stationary pi-electrons, while bonding *en passant*, the spins need to be opposite. When we add to the number of circulating pi-electrons and reduce the number at rest, we are increasing the magnitude of the spin quantum number S for the circulating set, while reducing the magnitude of S for the stationary set. The increasing disproportion that results may reduce the intrinsic probability of the electronic transition. This disproportion is only one of many contributions which need to be considered for the estimation of the transition probabilities of the different excitations which are energetically permitted.

I show in Fig. 12 the absorption lines resulting from the electronic excitations of the 19-bond and 16-bond loop currents. The display has been chosen to correspond to the display given earlier in Fig. 2. The energies shown are kinetic energies only, omitting the potential-energy adjustments discussed above. If I had included estimates for the potential-energy contributions, the theory would probably have matched the experiment more closely, with respect to the energy placement of the satellite absorption lines.

The experimental curve in Fig. 2 shows that the sets of three satellite peaks accompanying the blue peak and the red peak are very much smaller than these two main peaks. That is, excitations are most probable to the 9-electron, 19-bond, red peak and the 10-electron, 16-bond, blue peak. These excited states are evidently much more stable than their associated extra-electron excitations. To correlate these observations, we can consider a tentative generalization of the familiar Hückel stability rules discussed by Zimmerman [9]. These rules give stability to non-Möbius cyclic rings of $(4N+2)$ bonds and Möbius rings with $(4N)$ bonds, where N is an integer. For the tentative generalization, add the number of bonds in a loop, subtract the number of circulating electrons in a

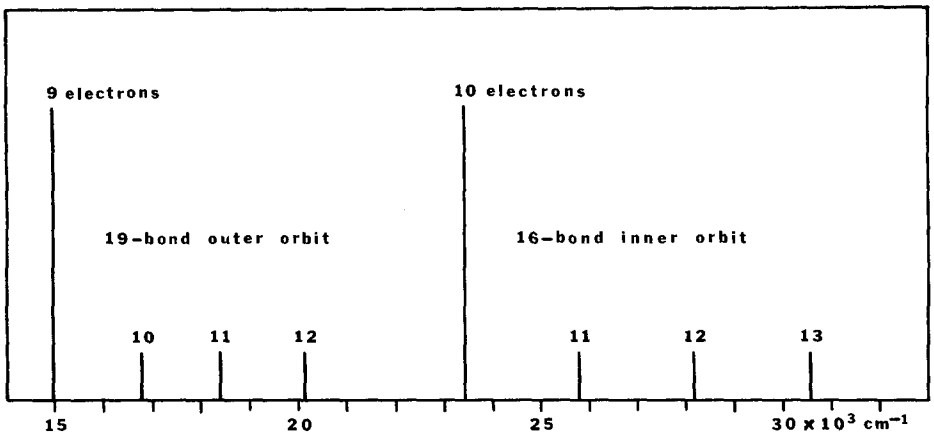

Fig. 12. Loop-current excitations in chlorophyll *a*, calculated from kinetic energies only. The energy scale is in wavenumber units, to correspond with the scale in Fig. 2

forward wave or add the number of circulating holes in a backward wave, and examine the result. If it has the form $(4N)$, a Möbius excitation should be stable. If it has the form $(4N+2)$, a non-Möbius excitation should be stable. By this formula, the Möbius ground state and the main red and blue excited states have enhanced stability, while the six satellite excitations do not. Accordingly, Fig. 12 shows the six satellite lines as much smaller than the two main lines, but this is very tentative and anticipatory.

The theoretical picture is very incomplete, particularly with respect to the oscillator strengths or transition probabilities. One qualitative feature of this loop-current picture stands out, however, in clear contrast with the molecular-orbital analysis of Christoffersen. In the loop-current picture there is a parallelism between the red absorption and the blue absorption. That is, the red absorption peak (the 9-electron excitation in the 19-bond orbit) is generalized to give satellite peaks (excitations of 10, 11, and 12 electrons traversing the same 19-bond orbit). Similarly, the blue absorption peak (the 10-electron excitation in the 16-bond orbit) is generalized to give satellite peaks (excitations of 11, 12, and 13 electrons traversing the same 16-bond orbit).

In contrast, the molecular-orbital theory of Christoffersen, as illustrated in Fig. 2, shows a very complicated line structure obtained from the theory for the blue and ultraviolet regions, and a too-simple line structure obtained from the theory for the red region. The parallelism of the loop-current picture is not present in the molecular-orbital theory of Christoffersen [7].

5. Magnetic Properties

The experimental observations are not limited to absorption spectra, but include in particular the measurements of magnetic circular dichroism illustrated in Fig. 7. While what is shown applies to a molecule which is not chlorophyll *a*,

the inner bond configurations are the same, so that the loop-current wave functions in Figs. 8–11 ought to apply directly to the molecule chlorin-e_6 trimethyl ester whose magnetic properties are shown in Fig. 7.

For these measurements the substance was dissolved in dioxane. The very strong magnetic field, 41.7 kilogauss, was produced by a superconducting magnet. In the loop-current picture, the ground state will be antiparamagnetic, with a positive charge circulating in a 19-bond Möbius orbit, and a portion of the molecular population will be aligned, at least in part, with the externally imposed magnetic field.

For the main red absorption peak, using the wave functions in Fig. 9, the excited state is characterized by $qL \doteq 1/2$, and the selection rule for radiative absorption then requires that the charge circulation in the excited state be opposite to the direction of circulation of the positive charge which moves in the Möbius ground state, where we also have $qL = 1/2$. This transition will preferentially absorb photons with left-handed polarization, leaving the right-handed ones to be observed as a positive MCD signal.

This is the positive deflection at 667 nm, at the right of Fig. 7. Let us pass over the structure in the middle right of the figure and move directly to the very strong signals in the 400 nm region. The positive peak at 420 nm has the same polarity as the 667 nm peak, and can be interpreted as a similar excitation to a state with $qL \doteq 1/2$, such as the 10-electron excited state illustrated through the wave functions in Fig. 11. But how then are we to account for the much stronger *negative* MCD signal which peaks at 395 nm?

One possibility is that the small amount of extra energy is enough to produce an excited state characterized by $qL \doteq 3/2$. Such a state is illustrated here in Fig. 13, where ten amplitude factors $E_{j'}$ are shown, similar to those in Fig. 11 and similarly taken from Eq. (18), but chosen here to have the quantum numbers $j' = 0$, 4, 8, 10, 12, 15, 17, 21, 25, 29. It can be seen that the electrons are crowded together in one region, and a calculation shows that the crowding represents an effective negative charge of about 1.54 units. These electrons are each circulating in an orbit with $L = 1$, so that the resultant state is close to $qL = 3/2$.

The transition from $qL = 1/2$ to $qL = 3/2$ is an allowed one for a radiative absorption, but now the charge circulation in the excited state is in the same sense as the ground-state positive-charge circulation, rather than in the opposite sense. The MCD signal is accordingly reversed, appearing as a large negative deflection at 395 nm in Fig. 7.

The next large deflection of the MCD curve (the solid curve) in Fig. 7 is the positive peak at 364 nm. This is positioned to correspond with a shoulder on the (dashed) absorption curve in the lower part of Fig. 7. From the interpretation suggested in Fig. 12, this is the wavelength region where an 11-electron excitation is dominant, within the inner 16-bond orbit. The MCD deflection is positive, indicating that the excited state is characterized by $qL \doteq 1/2$ rather than 3/2.

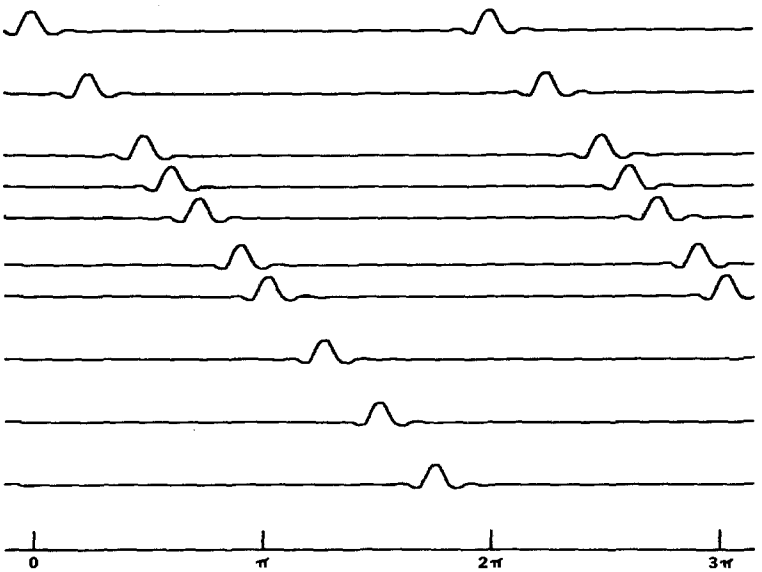

Fig. 13. The wave-function amplitudes $E_{j'}$ for $j' = 0, 4, 8, 10, 12, 15, 17, 21, 25, 29$. This is a 10-electron excitation with $qL \doteq 3/2$

Figure 14 shows a suggested 11-electron excited state, in which there is crowding in one region, similar to that of Fig. 13, but in addition there is one more electron inserted into the loop at a point about opposite to the region of crowding. The amplitude factors are again taken from Eq. (18), but now the quantum numbers

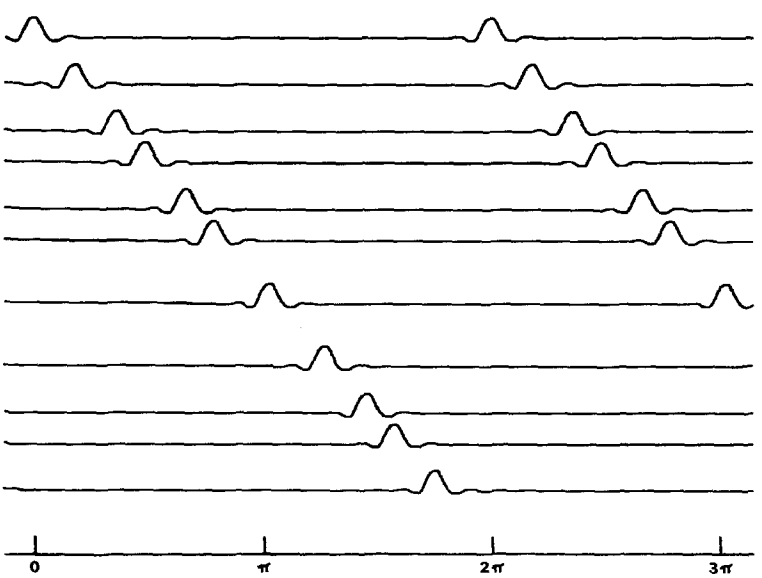

Fig. 14. The wave-function amplitudes $E_{j'}$ for $j' = 0, 3, 6, 8, 11, 13, 17, 21, 24, 26, 29$. This is an 11-electron excitation with $qL \doteq 1/2$

are $j' = 0, 3, 6, 8, 11, 13, 17, 21, 24, 26, 29$. The effective negative charge is about 0.47 units, consistent with $qL \doteq 1/2$.

The detailed explanation of measurements such as those in Fig. 7 will need to allow for vibrational energy. It can be seen from the electron crowding in Fig. 13 that this state with $qL \doteq 3/2$ will be throwing electrons back and forth, the recoil shaking the atomic framework. Energy is needed for this, and extra energy is indeed needed to produce this excitation, beyond the energy needed for the more even electron flow represented by Fig. 11.

Unanswered questions remain. What, for example, is causing the negative MCD signal at 534 nm? The corresponding absorption peak at 530 nm seems insignificant. Is there an electronic excitation which converts one sense of circular polarization into the other without absorbing either?

6. Triplet State

From studies of low-temperature phosphorescence in chlorophyll, it has been estimated that the energy level for the triplet state in chlorophyll *a* is about 930 nm, or 1750 cm^{-1} in wavenumber units. (See Seely [28], p. 17.) That is, there is a triplet state which stores less energy than that stored in the exciton, which is a singlet.

The biological utility of the singlet exciton lies in its capacity to deliver its stored energy in a package which moves with a single high-energy electron, as it is transferred down a chain of electron acceptors. A large fraction of the stored energy is utilized in the building of sugar molecules and in the formation of adenosine triphosphate. In the proposed model for an exciton there are nine electrons circulating around a 19-bond orbit. How can this distributed kinetic energy be so well tied to a single electron that it will move with that electron when it is transferred?

Of the 19 pi-electrons originally associated with the atoms in the 19-bond orbit, 9 are at rest and 9 are circulating. That leaves the 19th, which has moved to the center of the molecule. Figure 3(d) shows the central electron as coupled to the moving electrons in the Möbius ground state, particularly through the lower left nitrogen atom, the bottleneck through which all the loop-current circulations must pass. Figure 3(e) shows the excited state, with less coupling indicated, but the central electron could still be linked with the 9 circulating electrons in a spin state with all 10 spins parallel. This is a coupling via the exclusion principle which is reminiscent of the interaction between electron spins in a ferromagnet. In the present case we can call this a coupling between the magnetic moment of the central 19th electron and the magnetic field generated by the loop circulation of the 9 orbiting electrons, even while we recognize that the coupling is really a consequence of the exclusion principle operating among 10 electrons which all share a quantum state wherein nine move and one rests but each partakes of all so that all are interchangeable.

As long as the central electron remains in the same quantum state with the moving nine, it is in a position to carry with it the energy of the whole excitation. Its spin is pinned to the magnetic-field distribution carried by the 9-electron loop current. This picture suggests the answer to the question raised two paragraphs above. It is the exclusion principle which ties the distributed kinetic energy to a single electron.

If now the spin of that central electron were to be reversed, the ferromagnetic coupling would change and the energy of the molecule could be lowered. If the central-electron spin had been previously tightly tied into a combined system whose overall spin state was a singlet, then reversing the spin of the central electron would lead to a triplet state in which half of the triplet character was localized to the central region and the other half was distributed over the 19-bond orbit. Seely [28] reports that "The zero-field splitting parameter values indicate a very much delocalized electronic state" for the triplet state of chlorophyll as observed through ESR (electron spin resonance) measurements.

We can note in passing that the reversal of spin of the central electron, detaching it from the quantum state which it shared with the circulating nine electrons, will represent an increase in the entropy to be associated with this electronic excitation. Biological processes are intimately concerned with entropy, and low-entropy excitations are those which will be of value to living systems. A transition from a low-entropy singlet state to a high-entropy triplet state is doubly disadvantageous since it loses energy and acquires entropy. Evolution must have moved to discourage this transition, so inimical to life. Indeed, the chlorophyll triplet state is difficult to observe, and ordinarily requires that the experimenter work at 77°K, the temperature of liquid nitrogen, where living systems as we know them do not function well.

7. Discussion

The chlorophyll *a* monomers that serve as antennas in Photosystem I have certain biologically important excitations. They strongly absorb red photons and blue photons. Each absorbed solar photon is converted to an exciton which hops from one antenna chlorophyll to another, without fragmenting or reradiating, until it reaches a reaction center where its free energy is processed.

What I have examined here are certain electronic excitations within the porphyrin ring in chlorophyll *a*, excitations described in terms of loop currents. This description is a generalization of the free-electron molecular-orbital approach, a generalization in which each electron is represented as a wave packet built from Hückel orbitals. This generalization allows, in particular, a low-level Möbius excitation that would not easily be seen from the vantage point of the Hückel theory without wave packets.

I have tentatively identified electronic excitations that appear to correspond to the principal observed biological excitations. The low-level Möbius excitation is

proposed as the effective ground state *in vivo*. A nine-electron excited state using the outermost available ring of conjugated bonds is the proposed red excitation. This relaxes to a smooth nine-electron current flow which is the proposed exciton. The computed kinetic energies for the Möbius ground state and the nine-electron excited state give a close match to the observed red absorption peak, without the need to consider potential-energy contributions. There are three observed satellite absorption peaks next to the red peak. These can be associated with excited states involving 10, 11, and 12 circulating electrons within the same 19-bond orbit, but potential-energy contributions are needed to give the best fit between theory and experiment.

A ten-electron excited state using the innermost available ring of conjugated bonds is the proposed blue excitation. This 16-bond ring can also carry 11, 12, or 13 circulating electrons, and the three satellite absorption peaks next to the blue peak are explained in this way, while the 10-electron excitation accounts for the main blue peak at about 430 nm.

It may be possible to use these excited states to explain all the detailed observations of various kinds, such as CD, MCD, NMR, etc. If so, this will be a side benefit which serves to support the particular formulation. If the detailed explanations fail, here and there, the failures can be used in an effort to correct any explicit features of the theory that are flawed.

Sufficient support for the theoretical approach has already been presented here, it seems to me, to permit one to look further at the broader implications. The experimental curve in the upper part of Fig. 2 shows that biological selection has chosen a molecule with a rather simplified utilization of solar energy. While the molecule itself is elaborate enough to produce the theoretical spectrum in the lower part of Fig. 2, something about the molecule has introduced an element of simplicity in its actual functioning. The simplicity, I believe, lies in its utilization of low-entropy loop currents as the means for energy storage. The miscellaneous kinds of excitation suggested by the molecular-orbital calculations and shown in the lower part of Fig. 2 have in fact been shunted aside by the evolutionary process. Such complex spectral structures are seen in other molecules, but the molecule of preëminent importance to life has the simpler behavior.

The excitations of biological importance are those in which energy may involve many electrons, but the excitation has low entropy. The many electrons are participants in an excited state whose quantum-mechanical character ties these electrons tightly together. There is often a conversion process in which an excitation containing many moving electrons is translated into an excitation involving primarily a single electron. For this translation to be possible, the multi-electron excitation must have required high correlation among the moving electrons; it must have been a low-entropy excitation.

The chlorophyll excitations should be looked upon as important in their own right, but also as models or examples for many other low-entropy excitations of importance in biology.

Acknowledgement. Early support of this research program was provided by the U.S. Office of Naval Research, through Contract Nonr-778 (00), 1952–1954.

References

1. Platt, J. R. In: Radiation biology, ed. A. Hollaender, p. 71. New York: McGraw-Hill 1956
2. Kuhn, H.: J. Chem. Phys. **17**, 1198 (1949)
3. Simpson, W. T.: J. Chem. Phys. **17**, 1218 (1949)
4. Gouterman, M.: J. Chem. Phys. **30**, 1139 (1959)
5. Gouterman, M.: J. Chem. Phys. **33**, 1523 (1960)
6. Weiss, C., Jr.: J. Mol. Spectroscopy **44**, 37 (1972)
7. Christoffersen, R. E.: Int. J. Quant. Chem. **XVI**, 573 (1979)
8. Heilbronner, E.: Tetrahedron Letters **29**, 1923 (1964)
9. Zimmerman, H. E.: Quantum mechanics for organic chemists. New York: Academic Press 1975
10. Rabinowitch, E. I.: Photosynthesis. New York: Interscience 1945
11. Fischer, H.: Naturwissenschaften **26**, 401 (1940)
12. Geacintov, N. E., Van Nostrand, F., Pope, M., Tinkel, J. B.: Biochim. Biophys. Acta **226**, 486 (1971)
13. Geacintov, N. E., Van Nostrand, F., Becker, J. F. In: Proc. 2nd Int. Congr. Photosyn. Res., ed. G. Forti, M. Arton, A. Melandri, vol. i, p. 283. The Hague: W. Junk 1972
14. Geacintov, N. E., Van Nostrand, F., Becker, J. F., Tinkel, J. B.: Biochim. Biophys. Acta **267**, 65 (1972)
15. Breton, J., Michel-Villaz, M., Paillotin, G.: Biochim. Biophys. Acta **314**, 42 (1973)
16. Breton, J., Mathis, P. In: Excited states of biological molecules, ed. J. B. Birks, p. 301. New York: John Wiley and Sons 1976
17. Emsley, J. W., Feeney, J., Sutcliffe, L. H.: High resolution nuclear magnetic resonance spectroscopy. Oxford: Pergamon Press 1965
18. Vysotsky, Y. B., Kuzmitsky, V. A., Solovyov, K. N.: Theoret. Chim. Acta (Berl.) **59**, 467 (1981)
19. Maret, G., v. Schickfus, M., Mayer, A., Dransfeld, K.: Phys. Rev. Letters **35**, 397 (1975)
20. Briat, B., Schooley, D. A., Records, R., Bunnenberg, E., Djerassi, C.: J. Am. Chem. Soc. **89**, 6170 (1967).
21. Williams, W. P. In: Primary processes of photosynthesis, ed. J. Barber, p. 99. Amsterdam: Elsevier 1977
22. Murata, N., Nishimura, M., Takamiya, A.: Biochim. Biophys. Acta **126**, 234 (1966)
23. Paschenko, V. Z., Protasov, S. V., Rubin, A. B., Timofeev, K. N., Zamazova, L. M., Rubin, L. B.: Biochim. Biophys. Acta **408**, 143 (1975)
24. Bolton, J. R. In: Primary processes of photosynthesis, ed. J. Barber, p. 187. Amsterdam: Elsevier 1977
25. Clapp, R. E.: J. theor. Biol. **92**, 15 (1981)
26. Christophorou, L. G., McCorkle, D. L., Carter, J. G.: J. Chem. Phys. **60**, 3779 (1974)
27. Christophorou, L. G.: Atomic and molecular radiation physics. New York: Wiley-Interscience 1971
28. Seely, G. R. In: Primary processes of photosynthesis, ed. J. Barber, p. 1. Amsterdam: Elsevier 1977

Received October 2, 1981